

# Observing the Current Input in Neurons

**Pranay Goel**

Mathematical Biosciences Institute  
The Ohio State University  
231 W. 18th Avenue Columbus, Ohio 43210, USA  
Phone: +1-614-688-3493, Fax: +1-614-247-6643  
Email: pranay@mbi.osu.edu

**Klaus Röbenack**

Institut für Regelungs- und Steuerungstheorie  
Fakultät Elektrotechnik und Informationstechnik  
Technische Universität Dresden  
Mommsenstr. 13, 01099 Dresden, Germany  
Phone: +49-351-463-33421, Fax: +49-351-463-37281  
Email: klaus@roebenack.de

## Abstract

We propose a new technique that uses an observer to determine the current input into a neuron whose voltage is measured electrophysiologically. The current observer efficiently inverts the conductance-based model equations of the cell for the input, and also obtains the dynamics of the gating variables as a by-product. We show a version of the algorithm that is suitable for practical implementation. Theoretically, we prove the global convergence of the observer for all models of the Hodgkin-Huxley formalism. The current observer is accurate and can be implemented either offline or concurrently with the recording. It can potentially be useful even to *in vivo* recordings. We illustrate the workings of the observer on several neuronal models.

## 1 Introduction

Neurons communicate through synapses: *pre*-synaptic neuronal membrane activity is transmitted across the synapse via neurotransmitters that activate *post*-synaptic currents (PSCs) to drive the (postsynaptic) neuron. In order to fully understand the behavior of a neuron — whose membrane voltage can be recorded electrophysiologically — in the context of the surrounding network activity, it is necessary to know:

1. The ion channel kinetics underlying the dynamical makeup of the neuron,

2. The (synaptic, and applied) input current that drives it, and,
3. How subsequent downstream behavior is influenced.

Neurons exhibit subtle and complex membrane activity: an accurate determination of the input that drives this activity is essential to resolving the dynamics completely. However, the problem of determining the input current to neurons from the only available measurement — the membrane voltage — has not been fully explored.

Postsynaptic current *can* be determined in a purely experimental way (i.e., without first *modeling* the neuron mathematically): by voltage-clamping the neuron and measuring the PSC directly. (This, however, requires knowing the current corresponding to the clamping voltage in the absence of synaptic input; which can give rise to its own complications.) More significantly, except in the simplest circumstances, this procedure is intrinsically *invasive*: voltage-clamping the neuron will typically interfere with the network activity that the neuron is *participating* in. What is required is a sensor that passively reports the current input without interfering with the voltage activity.

On the other hand, significant effort is often expended in determining kinetic models for synaptic receptor dynamics. Typically, this involves recording PSC's generated by stimulating receptors with neurotransmitter in whole-cell, or excised patch-clamped experiments. Different Markov models are then proposed, whose reaction parameters are obtained to best fit this data. This is a useful step in simulating activity in networks of neurons. Nevertheless, in general this does not offer a solution for the *inverse* problem of determining synaptic dynamics *from* the measured activity. Moreover, this problem becomes more difficult as more complicated models of synaptic transmission are considered.

Techniques for determining kinetic models of ionic channels, proceeding from voltage and current clamping protocols, and “compartmental” models of neurons, are considerably mature [20]. Once a model for the neuron has been developed, a measurement of the time course of the voltage might be used to recover the (time-varying) input current. In other words, we consider designing an *observer* of the input when a part of the state of the neuron is known. An observer of the input only requires that the state equations of the neuron membrane be known; the estimate of the input is obtained independently of the details of the presynaptic dynamics. Thus, one need not obtain good models of synaptic transmission to implement the observer. (If such a model is available for some system, then that can be used to predict activity downstream of the neuron.)

Mathematical models describing membrane dynamics in neurons typically follow the formalism first described by Hodgkin and Huxley [16]. Briefly, the membrane voltage (difference) is given by a system of ODEs, where the *voltage* dynamics is coupled to several *gating* variables, which describe the behavior of the ion channels in the membrane.

$$C \frac{dV}{dt} = \sum_i \bar{g}_i m_i^{p_i} h_i^{q_i} (V_i - V) + I \quad (1a)$$

where each of the  $m_i$  and  $h_i$  satisfy equations of the form

$$\frac{dw}{dt} = a_w(V) (1 - w) - b_w(V) w \quad (1b)$$

with the summation taken over all the ionic channels in the cell. Each ionic channel is described by  $p_i$  activating gates, and  $q_i$  inactivating gates.  $V_i$  is the reversal potential for that channel, and  $\bar{g}_i$  is its maximal conductance.  $I$  is the current injected into the cell, whether applied via electrodes, or from pre-synaptic coupling to other cells,  $I = I_{syn} + I_{app}$ . Note that  $p_i$  and  $q_i$  are non-negative integral powers. If, for some channel neither  $p$  nor  $q$  are zero, then it describes a *transient* current. *Persistent* currents have  $q = 0$ , and *anomalous* or *hyperpolarization-activated* currents have  $p = 0$ . (Note that if  $p$  or  $q$  is 0, then it is meaningless to have an equation for the corresponding gating variable.) Furthermore, *passive* currents, such as a *leak* current, are described simply by  $g_L(V_L - V)$ .

From a control-theoretic point of view, system (1) is a single-input single-output state-space system with the input  $I$  and the state variables  $V$  and  $\mathbf{w} = (m_i, h_i)$ . The output  $V$  is measured. We propose a two-stage approach to reconstruct the input  $I$ . First, we design an observer to obtain the states  $\mathbf{w} = (m_i, h_i)$ . Second, we use the information provided by the observer to obtain an estimate of the input  $I$  using a filter.

An observer of (1) is a second dynamical system that reconstructs those quantities of (1) which are not measured. The problem of observer design has received significant attention during the last decades [32, 21, 23]. Classical observers provide an estimate of the state based on input and output information [23]. These observers are not applicable since the input  $I$  is not measured.

Extensions of observer theory have been made to systems with unmeasured inputs. These observers are called unknown input observers (UIO). The existence conditions for unknown input observers of linear time invariant systems are well-known. Several design procedures have been proposed in the literature [17, 29].

For nonlinear systems, the existence conditions of unknown input observers are not well established. Design methods exist only for special classes of nonlinear systems. The design method proposed in [22, 28] is based on a certain decomposition of the system into two subsystems. It turns out that systems of the class (1) are already decomposed into this special form. We will employ this approach to design an unknown input observer to estimate the unmeasured states  $\mathbf{w} = (m_i, h_i)$ .

The problem of observing an input occurs also in communication by chaotic signals [14]. In theory, we would use the inverse system approach suggested in [10, 11]. In this case, we had to differentiate the measured output numerically. Unfortunately, numerical differentiation by divided difference schemes is not reliable. To circumvent this problem, we will use an additional low-pass filter to generate a smoothed estimate of the input.

## 2 Observer and Filter Design

First, we will propose a reduced observer for system (2) to reconstruct the state variables which are not measured. Second, the desired current is estimated via an appropriate filtering scheme.

The class of models described by (1) has the form

$$C\dot{V} = f(V, \mathbf{w}) + I \quad (2a)$$

$$\dot{\mathbf{w}} = \mathbf{g}(V, \mathbf{w}), \quad \mathbf{w}(0) = \mathbf{w}_0 \in \mathbb{R}^p \quad (2b)$$

with the measured output  $V$  and the unknown initial value  $\mathbf{w}_0$ . The first subsystem (2a) is 1-dimensional, whereas the dimension  $p$  of the second subsystem (2b) depends on the model under consideration. System (2) is already in the Byrnes-Isidori normal form [4, 18]. In particular, the second subsystem (2b) depends not explicitly on the input  $I$ .

As an observer for  $\mathbf{w}$  we suggest a copy of subsystem (2b), which is driven by the measured output:

$$\dot{\hat{\mathbf{w}}} = \mathbf{g}(V, \hat{\mathbf{w}}), \quad \hat{\mathbf{w}}(0) = \hat{\mathbf{w}}_0. \quad (3)$$

The observation error  $\tilde{\mathbf{w}} = \mathbf{w} - \hat{\mathbf{w}}$  is governed by the error dynamics

$$\dot{\tilde{\mathbf{w}}} = \mathbf{g}(V, \mathbf{w}) - \mathbf{g}(V, \hat{\mathbf{w}}), \quad \tilde{\mathbf{w}}(0) = \hat{\mathbf{w}}_0 - \mathbf{w}_0. \quad (4)$$

The trajectory  $\hat{\mathbf{w}}$  of the observer (3) converges to the state  $\mathbf{w}$  of (2b) for  $t \rightarrow \infty$  if the equilibrium  $\tilde{\mathbf{w}} = \mathbf{0}$  of the error dynamics (4) is asymptotically stable uniformly in  $V$ . In other words, we assume that for all  $V$  we have

$$\mathbf{w}(t) - \hat{\mathbf{w}}(t) \rightarrow \mathbf{0} \quad \text{as } t \rightarrow \infty. \quad (5)$$

Then, subsystem (2b) is said to have a steady state solution property [2]. We will show in the appendix that the class of systems discussed here poses the property (5). Note that a system of the form (2), where the state of subsystem (2a) is measured and the subsystem (2b) has the property (5), is called detectable.

In contrast to conventional observers, we have no observer gain to adjust the convergence rate of the observer (3). Moreover, observer (3) is a reduced observer since we reconstruct only a subsystem of (2). Combining the measured  $V$  and the observer trajectory  $\hat{\mathbf{w}}$  yield an estimation of the whole state of (2), even though the input  $I$  is unmeasured. Therefore, the observation scheme used so far is a reduced unknown input observer.

Now, we make use of the information generated by the observer (3) to obtain an estimate of the current  $I$ . For known trajectories of  $V$  and  $\mathbf{w}$  we could compute the input  $I$  exactly from (2a) by

$$I = C\dot{V} - f(V, \mathbf{w}). \quad (6)$$

Since  $\mathbf{w}$  is not available directly but estimated by the observer (3), we consider an estimate  $\hat{I}$  of  $I$  defined by

$$\hat{I} = C\dot{V} - f(V, \hat{\mathbf{w}}). \quad (7)$$

For a continuous map  $f$  we have  $\hat{I}(t) \rightarrow I(t)$  for  $t \rightarrow \infty$  if  $\hat{\mathbf{w}}(t) \rightarrow \mathbf{w}(t)$  for  $t \rightarrow \infty$ , i.e., the estimation (7) converges to the exact input (6) provided the observer (3) converges to subsystem (2b).

In theory, we could estimate  $I$  by (7). This approach is used in [10, 11]. However, we measure  $V$  but not  $\dot{V}$ . A numerical computation of  $\dot{V}$  from  $V$  by divided differences

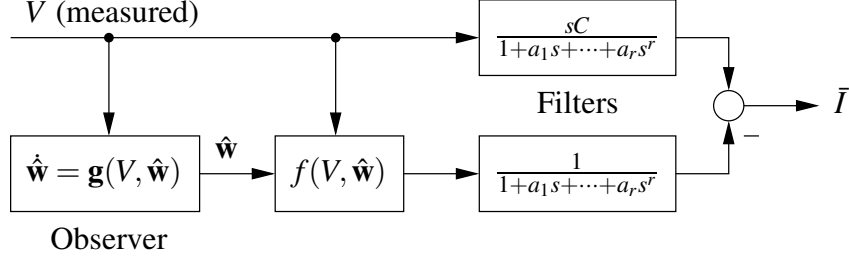


Figure 1: Reconstruction scheme for current  $I$  based on measurement of voltage  $V$ .

is not reliable. However, we can avoid an explicit computation of  $\dot{V}$  using a filter. More precisely, for the right hand side of (7) we use a continuous time low-pass filter with a transfer function

$$T(s) = \frac{1}{1 + a_1s + a_2s^2 + \dots + a_rs^r}, \quad r \geq 1, \quad (8)$$

where  $s$  is the complex variable used in connection with the Laplace transform. Of course, the coefficients  $a_1, \dots, a_r$  have to be chosen such that all poles of (8) are in the open left half plane. Otherwise, the filter would be unstable.

In the time domain, a filter given by (8) is a linear operator. In the following, we denote the action of a filter with the transfer function  $T$  on the signal  $\hat{I}$  by  $T \circ \hat{I}$ . The application of (8) to (7) yields the filtered signal

$$\bar{I}(t) = T(s) \circ \hat{I}(t) = C \cdot T(s) \circ \dot{V}(t) - T(s) \circ f(V(t), \hat{w}(t)). \quad (9)$$

Between  $V$  and its time derivative  $\dot{V}$  there holds  $\mathcal{L}\{\dot{V}\} = s\mathcal{L}\{V\} - V(-0)$ , where  $\mathcal{L}$  denotes the Laplace transform and  $V(-0)$  is the left-sided limit of  $V(t)$  at  $t = 0$ . For the design of the filter we assume that  $V(t) = 0$  for  $t < 0$ . (Even if  $V(-0) \neq 0$ , the influence of this value will fade away exponentially due to the filter.) Then, we have  $T(s) \circ \dot{V} \equiv sT(s) \circ V$ , i.e., instead of filtering the time derivative  $\dot{V}$  by (8) we filter the measured trajectory  $V$  by

$$\frac{s}{1 + a_1s + a_2s^2 + \dots + a_rs^r}. \quad (10)$$

Finally, the filtered estimate (9) is obtained by

$$\bar{I}(t) = sCT(s) \circ V(t) - T(s) \circ f(V(t), \hat{w}(t)). \quad (11)$$

The whole estimation scheme is shown in Fig. 1.

The purpose of the filter is to enhance the desired signal  $\hat{I}$  relative to disturbances such as noise. Here, the filtering is done on the basis of a suppression of selected frequencies to damp interfering signals. Since the current  $I$  is nearly constant, a natural choice for the filter is a low-pass. The most important parameter of a low-pass filter is its cut-off frequency  $\omega_0$ , at which the gain drops by some specified amount.<sup>1</sup>

<sup>1</sup>Note that the radian frequency  $\omega$  used for system-theoretic considerations and technical frequency  $f$  are linked by  $\omega = 2\pi f$ .

Although there are many possibilities to design a low-pass filter, in most applications Butterworth, Chebyshev and Cauer (or elliptic) filters are used [7].

The filters do not only damp the amplitude of selected frequencies, they also change the phase of the signals. This may lead to distortions of the wanted signal. In particular, the phase response of Cauer filters often results in strong distortions. Therefore, one may also consider the usage of Bessel filters, whose phase response results in a constant delay.

For both transfer functions (8) and (10), the numerator degree does not exceed the denominator degree. Hence, both filters can be implemented without differentiators. For our experiments we employed Butterworth low-pass filters.

### 3 Applications

We demonstrate the algorithm on some examples below.

The two models that we use below - the Hodgkin-Huxley equations and the Connor-Stevens equations — illustrate the two main types of excitability that have been classically identified in neurons: Type I and Type II ([15, 27], but see [19]). The two types of membranes can be distinguished by their different dynamics as the value of a (constant) injected current is increased. Type I excitability is mainly characterized by a saddle-node bifurcation that gives rise to oscillations that emerge with arbitrarily low *frequencies*; in Type II membranes a subcritical Hopf bifurcation leads to oscillations with arbitrarily low *amplitudes*.

#### 3.1 Hodgkin Huxley Model

The Hodgkin-Huxley [16] equations were first determined from the squid giant axon. We give the equations below:

$$C \frac{dV}{dt} = I - g_{Na} m^3 h (V - V_{Na}) - g_K n^4 (V - V_K) - g_L (V - V_L) \quad (12a)$$

$$\frac{dm}{dt} = a_m(V) (1 - m) - b_m(V) m \quad (12b)$$

$$\frac{dh}{dt} = a_h(V) (1 - h) - b_h(V) h \quad (12c)$$

$$\frac{dn}{dt} = a_n(V) (1 - n) - b_n(V) n \quad (12d)$$

with the functions

$$\begin{aligned} a_m(V) &= 0.1 (V + 40) / (1 - \exp(-(V + 40)/10)) \\ b_m(V) &= 4 \exp(-(V + 65)/18) \\ a_h(V) &= 0.07 \exp(-(V + 65)/20) \\ b_h(V) &= 1 / (1 + \exp(-(V + 35)/10)) \\ a_n(V) &= 0.01 (V + 55) / (1 - \exp(-(V + 55)/10)) \\ b_n(V) &= 0.125 \exp(-(V + 65)/80) \end{aligned} \quad (13)$$

and the parameters:  $V_{Na} = 50$  mV,  $V_k = -77$  mV,  $V_L = -54.4$  mV,  $g_{Na} = 120$  mS/cm<sup>2</sup>,  $g_k = 36$  mS/cm<sup>2</sup>,  $g_L = .3$  mS/cm<sup>2</sup>,  $C = 1$   $\mu$ F/cm<sup>2</sup>. Figure 2 below shows the steady states and oscillations as a function of the applied current: at low values of the current the membrane voltage is stable, as current is increased, the neuron fires repetitively. Notice that the oscillations first emerge with a non-zero frequency, which is characteristic of (the Hopf bifurcation in) the Type II membrane.

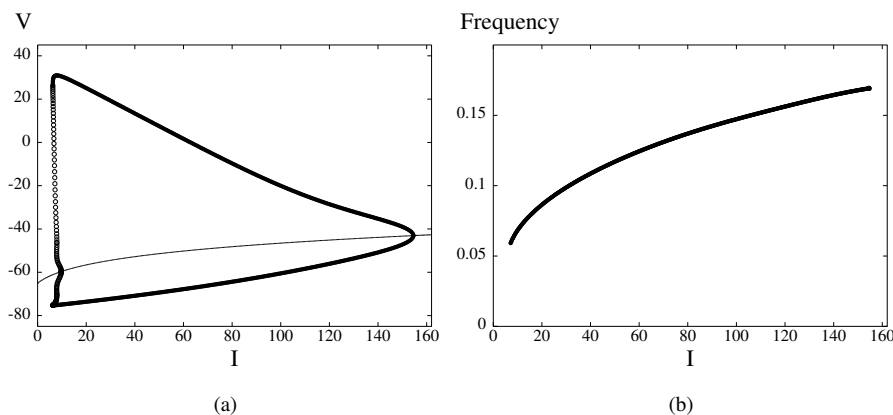


Figure 2: The membrane dynamics of the Hodgkin-Huxley neuron for fixed currents.

We consider simulation of system (12) with the initial values  $V(0) = -65$ ,  $m(0) = 0.05$ ,  $h(0) = 0.6$ , and  $n(0) = 0.317$ . Initially, a low value of background activity leaves the neuron close to its resting state. Suppose that at a time  $t=100$  ms, a stimulus arrives at the neuron, that kicks the neuron with a (tonic) excitation and induces a repetitive firing. Thus, in Fig. 3, a transition from rest to oscillation is induced by the current<sup>2</sup>

$$I(t) = \begin{cases} 5 & \text{for } 0 \text{ ms} \leq t \leq 100 \text{ ms} \\ 10 & \text{for } t > 100 \text{ ms.} \end{cases} \quad (14)$$

In the following, we will use the observation scheme described in Sect. 2 to estimate the current  $I$  based on the voltage  $V$ . The unknown input observer (3) consists of a copy of Eqns. (12b)-(12d) driven by the voltage  $V$  from (12a), that is

$$\begin{aligned} \dot{\hat{m}} &= a_m(V)(1 - \hat{m}) - b_m(V)\hat{m} \\ \dot{\hat{h}} &= a_h(V)(1 - \hat{h}) - b_h(V)\hat{h} \\ \dot{\hat{n}} &= a_n(V)(1 - \hat{n}) - b_n(V)\hat{n}. \end{aligned} \quad (15)$$

We use the zero vector as initial value for (15). It can be seen in Fig. 4 that the trajectories  $m$ ,  $h$ ,  $n$  of system (12) converge to the trajectories  $\hat{m}$ ,  $\hat{h}$ ,  $\hat{n}$  of the observer (15). This suggests that the subsystem (12b)-(12d) has indeed the steady-state solution property (5).

<sup>2</sup>The units of current are taken to be  $\mu$ A/cm<sup>2</sup> throughout the paper, and time is measured in msec.

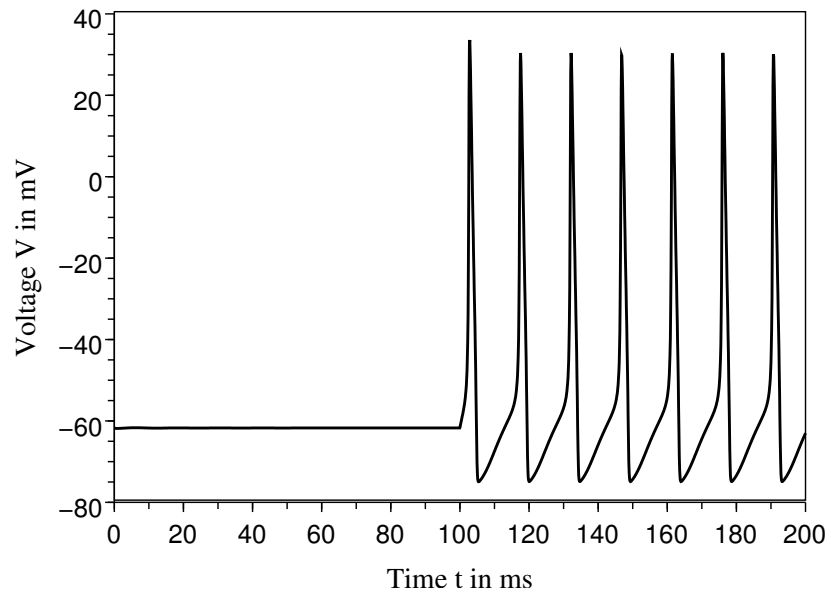


Figure 3: Voltage generated from model (12).

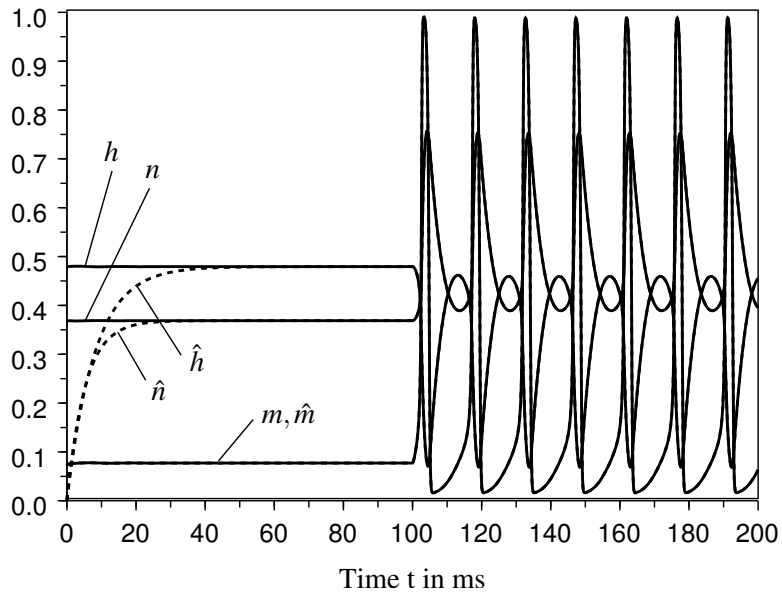


Figure 4: Trajectories of system (12) with the observer (15).

To estimate the current  $I$  by (11) we need to choose a low-pass filter and calculate its transfer function (8). We select a Butterworth filter of order  $r = 4$ , see [24]. In our numerical experiments we used three different filters with the (radian) cut-off frequencies  $\omega_0 = 1, 3$  and  $10$  rad/ms. Figure 5 shows the Bode plot of the associated three transfer functions. It can be seen that frequencies above the cut-off frequency are damped with approximately 80 dB per decade. The filter coefficients  $a_1, \dots, a_4$  are given in Tab. 1.

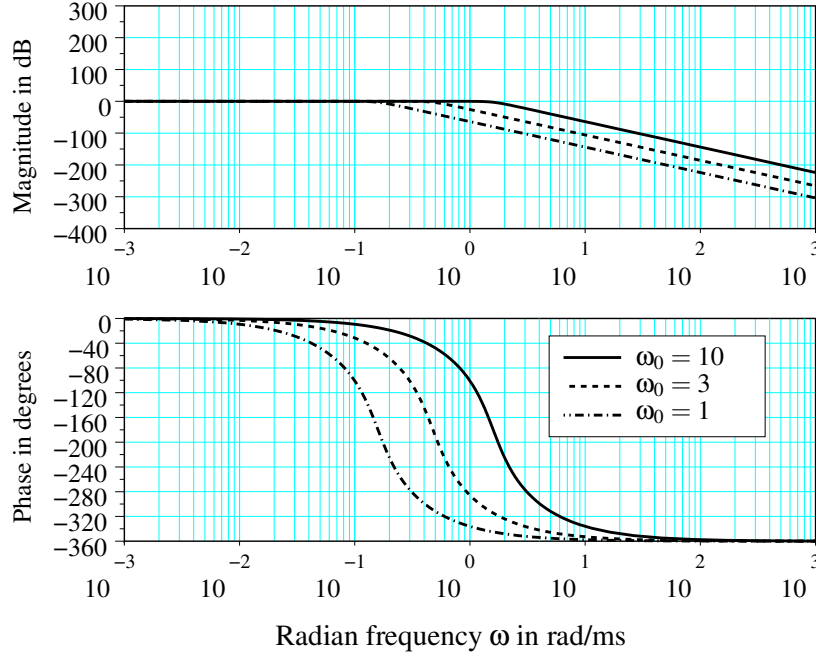


Figure 5: Bode plot of the three Butterworth filters.

	$\omega_0 = 1$	$\omega_0 = 3$	$\omega_0 = 10$
$a_1$	2.6131259	0.8710420	0.2613126
$a_2$	3.4142136	0.3793571	0.0341421
$a_3$	2.6131259	0.0967824	0.0026131
$a_4$	1.0000000	0.0123457	0.0001000

Table 1: Filter coefficients  $a_1, \dots, a_4$  for the time scale in ms.

Now we combine the unknown input observer (15) with the filter to estimate  $I$ . Figure 6 shows the filtered values  $\bar{I}$  generated by (11). The transient behavior of observer and filter result in relatively large amplitudes up to  $t \approx 20$  ms. For  $40 \text{ ms} \leq t \leq 100 \text{ ms}$  the filter basically yields the exact value of  $I = 5$ . The next interesting point is the jump of  $I$  at  $t = 100$  ms, for which the estimated values  $\bar{I}$  of  $I$  are plotted in Fig. 7. The highest cut-off frequency  $\omega_0 = 10$  of the filter results in fastest transients. A lower

cut-off frequency of the filter yields a smoother curve and is more suitable to suppress high-frequency noise.

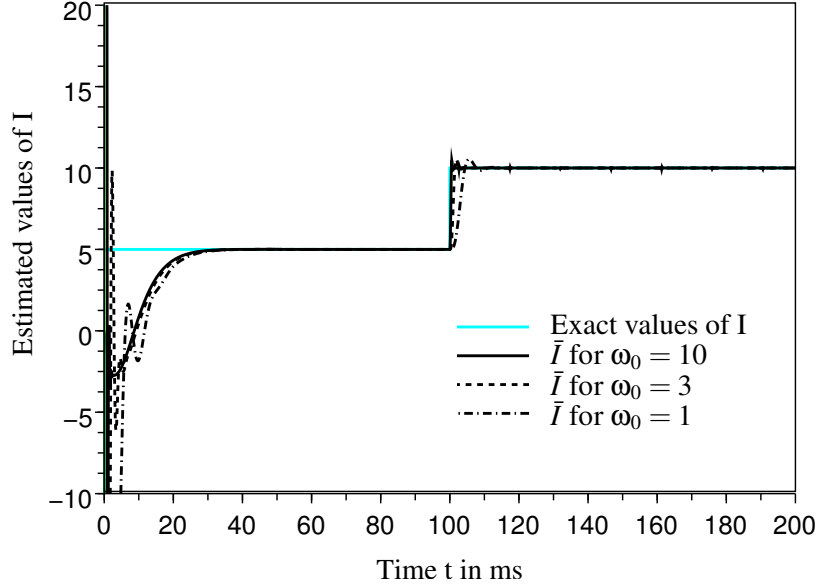


Figure 6: Estimated values of  $I$ .

### 3.2 Connor-Stevens Model

The Connor-Stevens [5] model is an example of a Type I membrane [8]:

$$C\dot{V} = -g_{Na}m^3h(V - V_{Na}) - g_Kn^4(V - V_K) - g_L(V - V_L) \quad (16a)$$

$$-g_Aa^3b(V - V_A) + I \quad (16b)$$

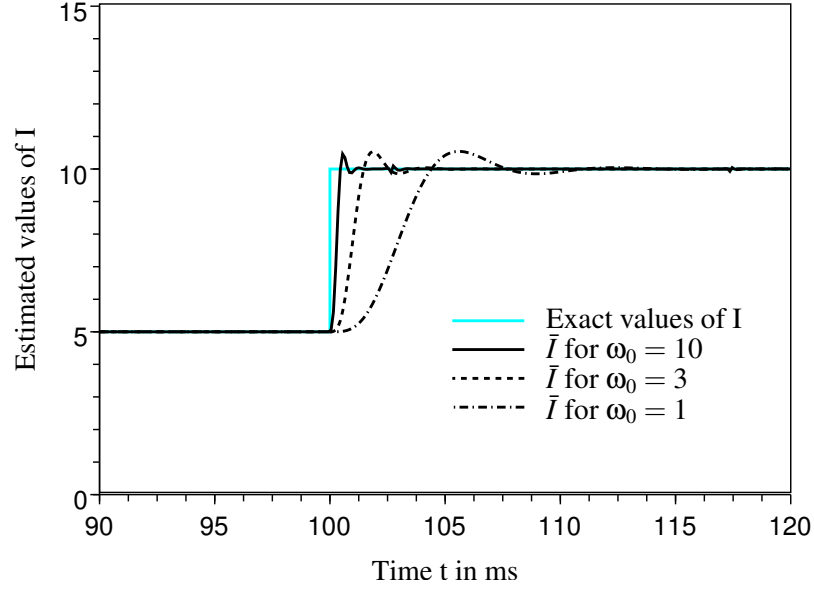
$$\dot{m} = \alpha_m(V)(1 - m) - \beta_m(V)m \quad (16c)$$

$$\dot{h} = \alpha_h(V)(1 - h) - \beta_h(V)h \quad (16d)$$

$$\dot{n} = \alpha_n(V)(1 - n) - \beta_n(V)n \quad (16e)$$

$$\dot{a} = \frac{a_\infty(V) - a}{\tau_a(V)} \quad (16f)$$

$$\dot{b} = \frac{b_\infty(V) - b}{\tau_b(V)} \quad (16g)$$

Figure 7: Estimated values of  $I$ .

with the functions

$$\begin{aligned}
 \alpha_m &= 0.38(V + 29.7)/1 - \exp(-0.1(V + 29.7)) \\
 \alpha_h &= 0.266 \exp(-0.05(V + 48)) \\
 \alpha_n &= 0.02(V + 45.7)/1 - \exp(-0.1(V + 45.7)) \\
 \beta_m &= 15.2 \exp(-0.0556(V + 54.7)) \\
 \beta_h &= 3.8/(1 + \exp(-0.1(V + 18))) \\
 \beta_n &= 0.25 \exp(-0.0125(V + 55.7)) \\
 a_\infty &= \left( \frac{0.0761 \exp(0.0314(V + 94.22))}{1 + \exp(0.0346(V + 1.17))} \right)^{1/3} \\
 \tau_a &= 0.3632 + 1.158/(1 + \exp(0.0497(V + 55.96))) \\
 b_\infty &= \left( \frac{1}{1 + \exp(0.0688(V + 53.3))} \right)^4 \\
 \tau_b &= 1.24 + 2.678/(1 + \exp(0.0624(V + 50)))
 \end{aligned}$$

and with the parameters:  $V_{Na} = 55$  mV,  $V_k = -72$  mV,  $V_L = -17$  mV,  $V_A = -75$  mV,  $C = 1$   $\mu$ F/cm<sup>2</sup>,  $g_{Na} = 120$  mS/cm<sup>2</sup>,  $g_k = 20$  mS/cm<sup>2</sup>,  $g_L = 0.3$  mS/cm<sup>2</sup>,  $g_A = 47.7$  mS/cm<sup>2</sup>.

Figure 8 below shows the firing rate characteristics of the Connor-Stevens membrane. Notice the saddle-node (on an invariant circle) bifurcation that is characteristic of a Type I membrane: the neuron can fire with an arbitrary latency.

The initial values are  $V(0) = -64.453$ ,  $m(0) = 0.0159$ ,  $h(0) = 0.9437$ ,  $n(0) = 0.196$ ,  $a(0) = 0.0559$ ,  $b(0) = 0.2175$ . We use a similar current signal as in Sect. 3.1,

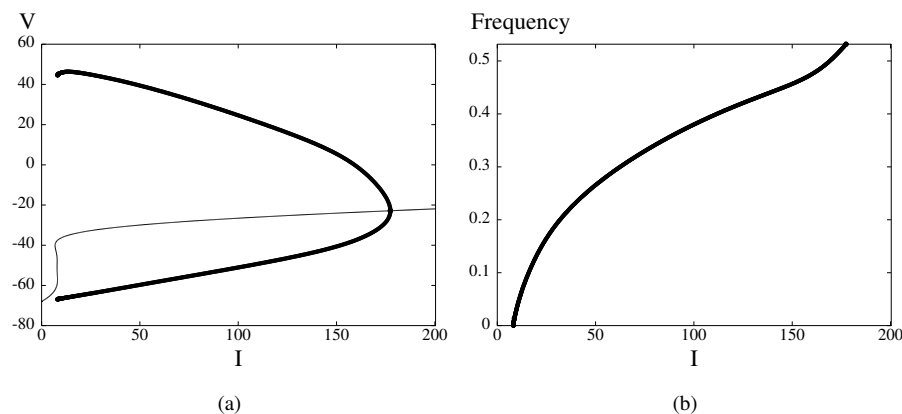


Figure 8: The membrane dynamics of the Connor-Stevens neuron.

namely

$$I(t) = \begin{cases} 5 & \text{for } 0 \text{ ms} \leq t \leq 100 \text{ ms} \\ 12 & \text{for } t > 100 \text{ ms.} \end{cases} \quad (17)$$

The associated voltage signal is shown in Fig. 9.

The measured voltage of the Connor-Stevens model (16) is used to reconstruct the other state variables  $m$ ,  $h$ ,  $n$ ,  $a$ , and  $b$ . The unknown input observer (3) consists of Eqns. (16c) to (16g), which are driven by the voltage  $V$ . The state variables of the observer are denoted by  $\hat{m}$ ,  $\hat{h}$ ,  $\hat{n}$ ,  $\hat{a}$ , and  $\hat{b}$ , respectively. Since we have no further knowledge of these variables at  $t = 0$ , we use the zero vector of  $\mathbb{R}^5$  as an initial value of the observer. It can be seen in Fig. 10 that the original trajectories of (16c) to (16g) converge to the trajectories of the associated observer.

Next, we used a 4th order Butterworth low-pass filter according to (11) to estimate the current. The result is shown in Fig. 11. After some transients we obtain an exceptionally good estimate  $\bar{I}$  of  $I$ .

### 3.3 An Illustrative Example from Population Oscillations in Neuronal Networks

A firing-rate curve such as those in Figs. 2(b) and 8(b) often serves as a convenient index of neuronal activity as a function of average *tonic* input to the neuron. However, measuring activity in terms of a firing *rate* suffers from the drawback that when single spikes may carry meaningful information, a definition of "rate" is meaningless. Moreover, if the current is transient, then tracing activity along the F-I curve is not particularly accurate either.

Figure 12 shows a case where a casual measurement of firing *frequency* does not determine the input drive unambiguously. In the two cases shown in Fig. 12, the frequency of firing is very nearly similar; the input current, however, is very different.

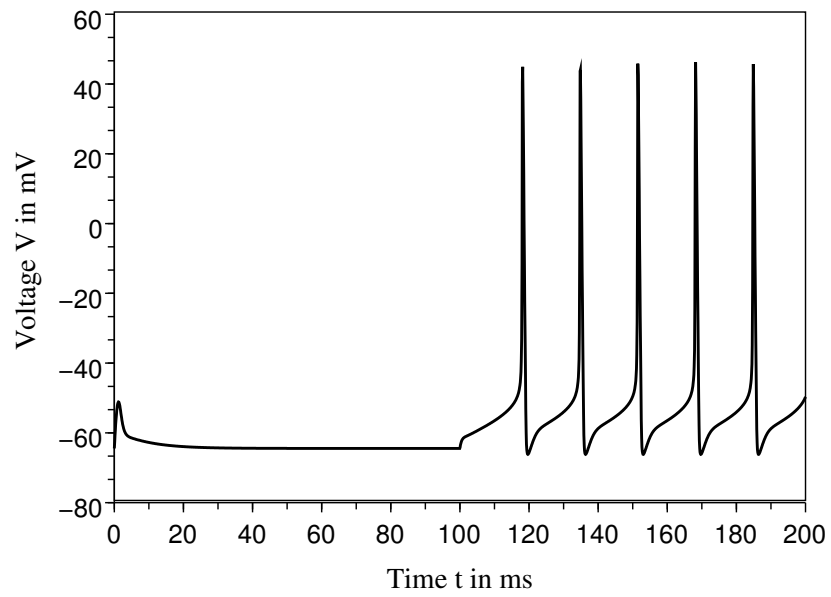


Figure 9: Voltage generated from the Connor-Stevens model (16).

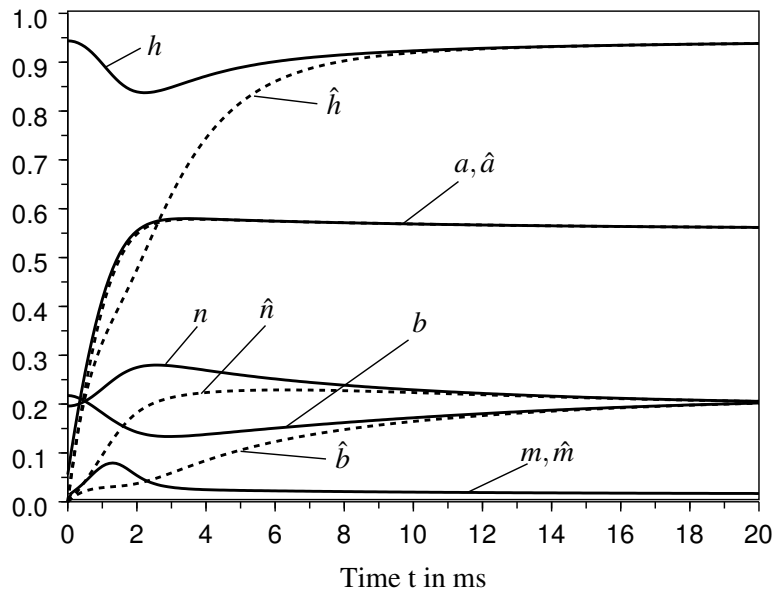


Figure 10: Trajectories of Connor-Stevens model (16) and the unknown input observer.

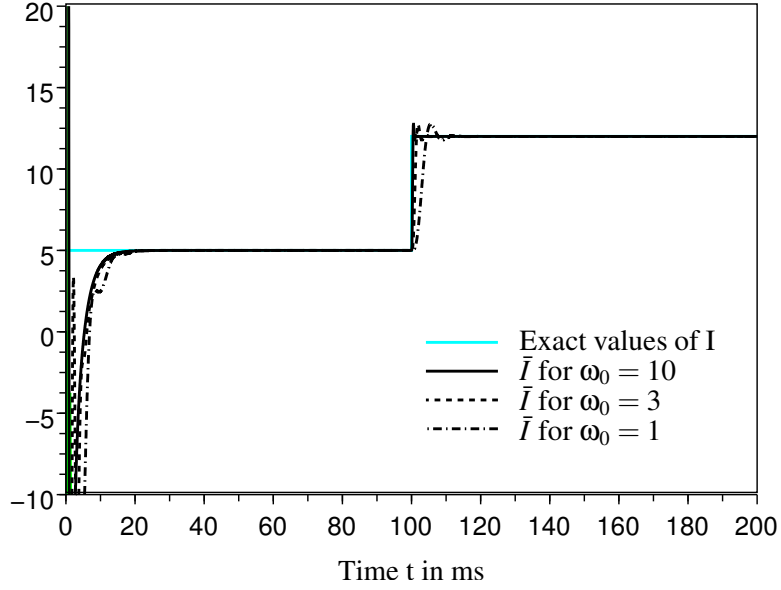


Figure 11: Estimated current for the Connor-Stevens model (16).

In one case the neuron is driven by a constant current. In the other case, the input is time-varying: such an input may arise, for example, from another similar neuron that might be synchronized with the former (see [30] for an example of brain rhythms).

Synchronicity, and spatio-temporal spiking patterns in general [9], often give clues to theoreticians about the exact nature of connectivities between different neurons in a tissue, and ultimately to the computation being performed in the network. Computer simulations, however, usually tend to make (simplifying) assumptions about the nature of the drive that excites activity. Current observers can supplement theoretical reasoning by investigating the (changing) inputs directly.

We illustrate this section with the Traub model [31]:

$$\begin{aligned}
 C \frac{dV}{dt} &= I - g_{Na} m^3 h (V - V_{Na}) - g_K n^4 (V - V_K) - g_L (V - V_L) - g_{AHP} w (V - V_K) \\
 \frac{dm}{dt} &= a_m(V) (1 - m) - b_m(V) m \\
 \frac{dh}{dt} &= a_h(V) (1 - h) - b_h(V) h \\
 \frac{dn}{dt} &= a_n(V) (1 - n) - b_n(V) n \\
 \frac{dw}{dt} &= \frac{w_\infty(V) - w}{\tau_w(V)}
 \end{aligned} \tag{18}$$

with the functions

$$\begin{aligned}
 a_m(V) &= 0.32(54 + V)/(1 - \exp(-(V + 54)/4)) \\
 b_m(V) &= 0.28(V + 27)/(\exp((V + 27)/5) - 1) \\
 a_h(V) &= 0.128 \exp(-(50 + V)/18) \\
 b_h(V) &= 4/(1 + \exp(-(V + 27)/5)) \\
 a_n(V) &= 0.032(V + 52)/(1 - \exp(-(V + 52)/5)) \\
 b_n(V) &= 0.5 \exp(-(57 + V)/40) \\
 w_\infty(V) &= \frac{1}{1 + \exp(-(V + 35)/10)} \\
 \tau_w(V) &= \frac{400}{3.3 \exp((V + 35)/20) + \exp(-(V + 35)/20)}
 \end{aligned}$$

and with the parameters:  $V_{Na} = 50$  mV,  $V_k = -100$  mV,  $V_L = -67$  mV,  $C = 1$   $\mu$ F/cm<sup>2</sup>,  $g_{Na} = 100$  mS/cm<sup>2</sup>,  $g_k = 80$  mS/cm<sup>2</sup>,  $g_L = 0.1$  mS/cm<sup>2</sup>,  $g_{AHP} = 0.3$  mS/cm<sup>2</sup>. Using the observer filter scheme, it is easily determined if the input is oscillatory (phasic) or tonic, even though the measured voltages have similar frequencies (Fig. 12).

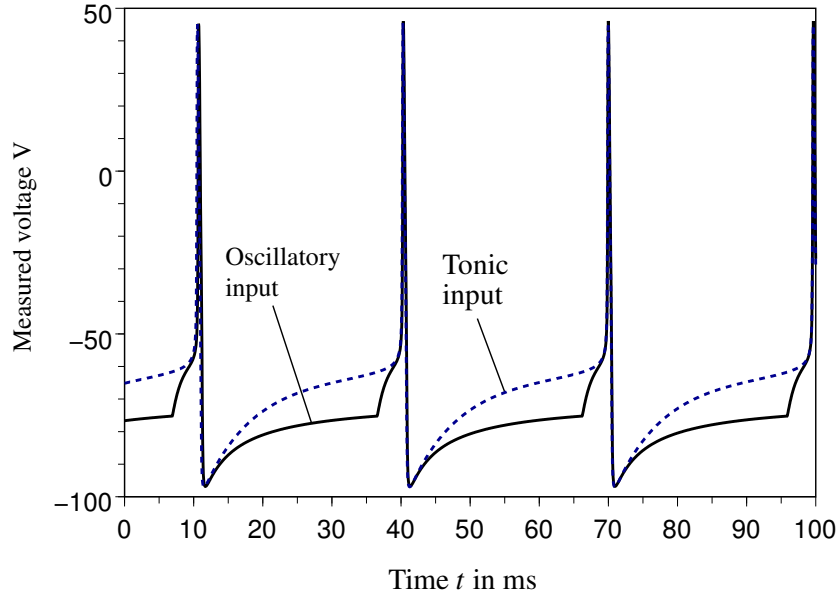


Figure 12: Two responses of the Traub equations with similar frequencies, but different drives.

First, we consider model (18) with the time-varying current shown in Fig. 13 and the initial values  $V(0) = -76.65$ ,  $m(0) = 0.0018$ ,  $h(0) = 0.99$ ,  $n(0) = 0.006$ ,  $w(0) = 0.1$ . Our aim is the reconstruction of this current from measured voltage  $V$ . In addition to the observer (3) we used a 4th order Butterworth low-pass filter. The cut frequency

should be significantly higher than the frequency of the expected signal. We have chosen  $\omega_0 = 10$  rad/ms. The reconstructed input  $\bar{I}$  generated by the filter is shown in Fig. 13. The filter output  $\bar{I}$  matches the real current  $I$  well.

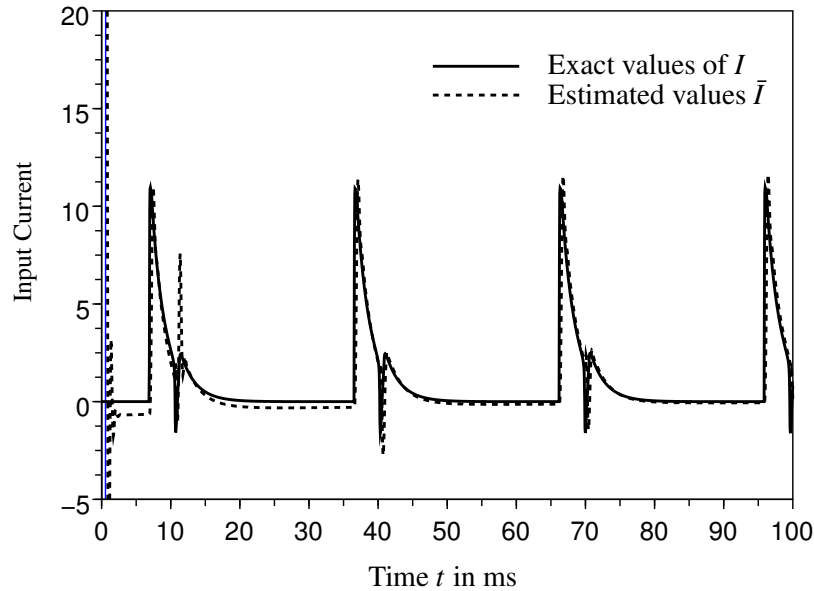


Figure 13: Input Current for the Traub model - variant 1.

In the second case we consider a constant input current  $I = 2$ . We used the initial values  $V(0) = -76.65$ ,  $m(0) = 0.0018$ ,  $h(0) = 0.99$ ,  $n(0) = 0.006$ ,  $w(0) = 0.1$ . We applied the same observer filter constellation as for the oscillatory input. The exact current  $I$  and the reconstructed current  $\bar{I}$  are shown in Fig. 14. Although  $\bar{I}$  is going together with  $I$ , there are some differences in the beginning. In particular, there are spikes at  $t \approx 12$ , 40 and 70 ms, and visible differences in between. These effects are caused by the error dynamics (4) of the observer. The spikes shall be avoided if one uses a lower cut-off frequency of the filter since the convergence rate of the associated observer (3) cannot be increased.

## 4 Discussion

A direct measurement of the synaptic input driving a neuron, especially *in vivo*, is a challenging problem. We have presented here a technique useful for determining the current input into a neuron whose membrane voltage is measured directly. The algorithm implements the inversion of the compartmental equations (1) for the input  $I$ . While we have taken this input to be a synaptic current (driving, say, a somatic compartment) for the purposes of this paper, the exact interpretation of this input depends on the context in which the compartment is being modeled. The input term may be, for example, a gap junctional current,  $g_{gap}(V_n - V)$ , where  $V_n$  is the voltage of the

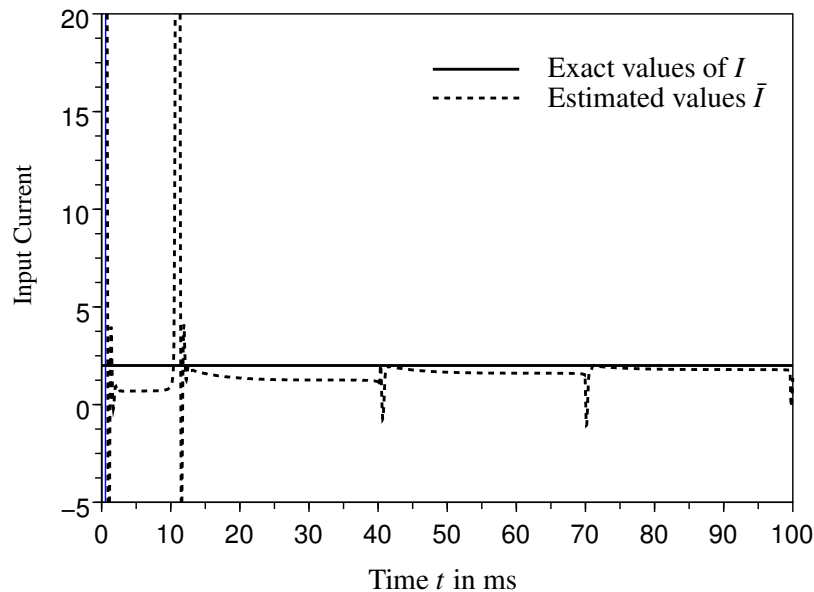


Figure 14: Input Current for the Traub model - variant 2.

neighboring cell and  $g_{gap}$  represents diffusive coupling (a similar form applies to coupling between compartments). Future work will also consider the extension of current observer design to multi-compartmental models.

Observers for synaptic current can be used to implement a sensor with a minimal of interference *in vivo*. Theoretically, they solve the inverse problem of determining the input from a partial measurement of the state (here, the membrane voltage). Additionally, the observer also recovers the time courses of the gating variables which cannot be directly measured. Such a capability clearly enlarges the scope of useful information that can be obtained from electrophysiological recordings. An observer for synaptic current can be used quite generally in any context that a neuron is recorded from, and especially effectively in studying small networks. They can have a variety of practical applications.

*Current Observers and Synaptic Plasticity.* Learning, memory and plasticity in neuronal networks are among the outstanding problems that have occupied neuroscientists for several decades. Hebb's celebrated postulate holds synaptic plasticity as the locus of enduring change arising as a consequence of network activity [3]. There are several examples of synaptic and non-synaptic plasticity (see [1, 6] for reviews) that have been studied in the context of network dynamics. An immense body of (mostly theoretical) work typically concerns itself with computations performed by changing synaptic weights in networks of "neurons" whose intrinsic excitability is presumed unaltered. An observer of synaptic current opens up the potential of not only a direct qualitative verification of a Hebbian hypothesis (in some given system), but also a *quantitative* one. Another example of such a scenario lies with studying associative

conditioning. Conditioning trials repeatedly pair applications of conditional stimuli with unconditional stimuli; neurons along, and at the sites of convergence of the two pathways, might be systematically probed for changes in synaptic currents that are associated with the learning behavior.

In a modeling cycle concerning neurons, techniques for determining kinetic models of ionic channels, and conductance-based models after the fashion of Hodgkin and Huxley, have matured considerably. On the other hand, mathematical analyses of the dynamical properties of neurons continue to provide considerable understanding of the behavior of neuronal networks from a theoretical point of view. Current observers can potentially be used for a direct and independent verification of theoretical models. Dynamic clamping [26] uses computer simulation to introduce artificial membrane or synaptic conductances into biological neurons. It has been used to create hybrid circuits coupling real and artificial neurons. The technique of effective current observers promises to bridge the gap between speculative theoretical modeling and direct experiment even further.

## Acknowledgement

P. Goel would like to acknowledge that this material is based upon work supported by the National Science Foundation under Agreement No. 0112050. K. R obenack was supported by Deutsche Forschungsgemeinschaft under research grant RO 2427/1.

## Appendix

We show here that the observer designed in (3) is globally asymptotically stable. We also claim that this observer is applicable to *all* models of the Hodgkin-Huxley type.

The Markov model of an ionic channel is given by:



Thus, the probability that the  $i^{\text{th}}$  channel is in the open state,  $w_i$ , is given by

$$\frac{dw_i}{dt} = a_i(V) w_i - b_i(V) (1 - w_i) \quad (20)$$

where the rates  $a_i(V), b_i(V) > 0$ . Thus each equation of the subsystem (2b) obeys an equation of the form (dropping the subscript  $i$  for simplicity):

$$\begin{aligned} \dot{w} &= a(V)(1 - w) - b(V)w \\ &= a(V) - (a(V) + b(V))w \\ &= a(V) - \gamma(V)w \end{aligned} \quad (21)$$

where  $\gamma(V) = a(V) + b(V) > 0$ . The corresponding observer obeys

$$\dot{\hat{w}} = a(V) - \gamma(V)\hat{w}, \quad \hat{w}(0) = \hat{w}_0, \quad (22)$$

which is a copy of (21) excited by the measured  $V$ . The observation error,  $\tilde{w} = w - \hat{w}$ , is then given by

$$\dot{\tilde{w}} = \dot{w} - \dot{\hat{w}} = -\gamma(V)\tilde{w}, \quad \tilde{w}(0) = w_0 - \hat{w}_0. \quad (23)$$

The candidate Lyapunov function  $\mathcal{V}(\tilde{w}) = \frac{1}{2}\tilde{w}^2$  is continuously differentiable, positive definite and radially unbounded. Its total derivative along the error dynamics (23) reads as

$$\dot{\mathcal{V}}(\tilde{w}) \Big|_{(23)} = \tilde{w}\dot{\tilde{w}} = -\gamma(V)\tilde{w}^2 < 0 \quad \forall \tilde{w} \neq 0.$$

Hence, by Lyapunov's Theorem [12], the equilibrium  $\tilde{w} = 0$  of (23) is globally asymptotically stable, i.e.,  $\tilde{w}(t) \rightarrow 0$  for  $t \rightarrow \infty$  and any initial value  $\tilde{w}(0) \in \mathbb{R}$ . This implies  $\hat{w}(t) \rightarrow w(t)$  for  $t \rightarrow \infty$ , that is, the trajectory  $\hat{w}(t)$  of the observer (22) converges to the trajectory  $w(t)$  of the original system (21) for  $t \rightarrow \infty$ .

Define the number  $\gamma_0$  by  $\gamma_0 = \inf_{V \in \mathbb{R}} \gamma(V)$ . If in addition  $\gamma_0 > 0$ , then the equilibrium  $\tilde{w} = 0$  is globally exponentially stable, where  $\gamma_0$  denotes the convergence rate. In this case we have  $|\tilde{w}(t)| \leq |\tilde{w}(0)|e^{-\gamma_0 t}$  for all  $t \geq 0$ , see [13].

Since the transition rates  $a(V)$  and  $b(V)$  in (19) are positive for *all* systems that obey the Hodgkin-Huxley formalism, from the argument give here (equation (23)) it follows that observer constructed above is convergent for any (such) neuronal model. Moreover, the equation (21) can equivalently be written as  $\dot{w} = (w_\infty(V) - w)/\tau_w(V)$ , where  $w_\infty(V) = a(V)/(a(V) + b(V))$  and  $\tau_w(V) = 1/(a(V) + b(V))$ , which indicates that for a fixed  $V$ ,  $w$  approaches the limiting value  $w_\infty(V)$  with a time constant  $\tau_w(V)$ . From this form it is apparent that  $\gamma(V) = 1/\tau_w(V)$ .

## References

- [1] Abbott LF, Nelson SB. Synaptic plasticity: taming the beast. *Nat Neurosci*, 3 Suppl:1178–1183, Nov 2000.
- [2] Amicucci GL, Monaco S. On nonlinear detectability. *J. Franklin Inst.*, 335B(6):1105–1123, 1998.
- [3] Brown RE, Milner PM. The legacy of Donald O. Hebb: more than the Hebb synapse. *Nat Rev Neurosci*, 4(12):1013–1019, Dec 2003. Biography.
- [4] Byrnes CI, Isidori A. Asymptotic stabilization of minimum phase nonlinear systems. *IEEE Trans. on Automatic Control*, 36(10):1122–1137, 1991.
- [5] Connor JA, Stevens CF. Prediction of repetitive firing behaviour from voltage clamp data on an isolated neurone soma. *Journal of Physiology*, 213:31–53, 1971.
- [6] Daoudal G, Debanne D. Long-term plasticity of intrinsic excitability: learning rules and mechanisms. *Learn Mem*, 10(6):456–465, Nov 2003.
- [7] Denbig P. *System Analysis & and Signal Processing*. Addison-Wesley, 1998.
- [8] Ermentrout B. Type I membranes, phase resetting curves, and synchrony. *Neural Comput*, 8(5):979–1001, Jul 1996.

- [9] Ermentrout GB. Neural networks as spatio-temporal pattern-forming systems. *Report on Progress in Physics*, 64:353–430, 1998.
- [10] Feldmann U. *Synchronization of Chaotic Systems*. PhD thesis, Technische Universität Dresden, 1995.
- [11] Feldmann U, Hasler M, Schwarz W. Communication by chaotic signals: the inverse system approach. *Int. J. of Circuit Theory and Applications*, 24(5):551–579, 1996.
- [12] Guckenheimer J, Holmes P. *Nonlinear oscillations, dynamical systems, and bifurcations of vector fields*, volume 42 of *Applied Mathematical Sciences*. Springer-Verlag, New York, 1990. Revised and corrected reprint of the 1983 original.
- [13] Hahn W. *Stability of Motion*. Springer-Verlag, 1967.
- [14] Hasler M. Engineering chaos for encryption and broadband communication. *Philosophical Transactions of the Royal Society of London, series A*, 353:115–126, 1995.
- [15] Hodgkin AL. The local electric changes associated with repetitive action in a non-medulated axon. *J. Physiol. (London)*, 107:165–181, 1948.
- [16] Hodgkin AL, Huxley AF. A quantitative description of membrane current and its application to conduction and excitation in nerve. *Journal of Physiology*, 117:500–544, 1952.
- [17] Hostetter GH, Meditch JS. On the generalization of observers to systems with unmeasurable, unknown inputs. *Automatica*, 9:721–724, 1973.
- [18] Isidori A. *Nonlinear Control Systems: An Introduction*. Springer-Verlag, London, 3rd edition, 1995.
- [19] Izhikevich EM. Neural excitability, spiking, and bursting. *International Journal of Bifurcation and Chaos*, 10:1171–1266, 2000.
- [20] Johnston D, Wu SM. *Foundations of Cellular Neurophysiology*. MIT Press, Cambridge, MA, 1995.
- [21] Misawa EA, Hedrick JK. Nonlinear observers — a state-of-the art survey. *Journal Dynamic Systems, Measurement, and Control*, 111:344–352, September 1989.
- [22] Moreno J. Unknown input observers for SISO nonlinear systems. In *CDC 2000*, volume 1, page 790, 2000.
- [23] Nijmeijer H, Fossen TI, editor. *New Directions in Nonlinear Observer Design*, volume 244 of *Lecture Notes in Control and Information Science*. Springer-Verlag, 1999.

- [24] Parks TW, Burrus CS. *Digital Filter Design*, chapter 7. John Wiley & Sons, New York, 1987.
- [25] Pernarowski M. Controllability of excitable systems. *Bull Math Biol*, 63(1):167–184, Jan 2001.
- [26] Prinz AA, Abbott LF, Marder E. The dynamic clamp comes of age. *Trends Neurosci*, 27(4):218–224, Apr 2004.
- [27] Rinzel J, Ermentrout B. Analysis of neural excitability and oscillations. In *Methods in Neuronal Modeling: From Synapses to Networks*, pages 251–292. MIT Press, Cambridge, MA, 1998.
- [28] Rocha-Cózatl E, Moreno J. Passivity and unknown input observers for nonlinear systems. In *15th Triennial World Congress of the International Federation of Automatic Control Barcelona, 21-26 July 2002*, 2002.
- [29] Sundareswaran KK, McLane PJ, Bayoumi MM. Observers for linear systems with arbitrary plant disturbances. *IEEE Trans. on Automatic Control*, AC-22(5):870–871, October 1977.
- [30] Traub RD, Jefferys JGR, Whittington M. *Fast Oscillations in Cortical Circuits*. MIT Press, Cambridge, MA, 1999.
- [31] Traub RD, Miles R. *Neuronal networks of the hippocampus*. Cambridge University Press, Cambridge, 1991.
- [32] Walcott BL, Corless MJ, Žak SH. Comparative study of non-linear state-observation techniques. *Int. J. Control*, 45(6):2109–2132, 1987.